Constraints on primordial non-Gaussianity from WMAP7 and luminous red galaxies power spectrum and forecast for future surveys

Francesco De Bernardis,[1,2] Paolo Serra,[2] Asantha Cooray,[2] and Alessandro Melchiorri[1]

[1]*Physics Department and INFN, Universita' di Roma "La Sapienza," Ple Aldo Moro 2, 00185, Rome, Italy*

[2]*Center for Cosmology, Department of Physics & Astronomy, University of California Irvine, Irvine, California 92697, USA*

(Received 17 May 2010; published 8 October 2010)

We place new constraints on the primordial local non-Gaussianity parameter $f_{\rm NL}$ using recent cosmic microwave background anisotropy and galaxy clustering data. We model the galaxy power spectrum according to the halo model, accounting for a scale-dependent bias correction proportional to $f_{\rm NL}/k^2$. We first constrain $f_{\rm NL}$ in a full 13 parameters analysis that includes 5 parameters of the halo model and 7 cosmological parameters. Using the WMAP7 CMB data and the SDSS DR4 galaxy power spectrum, we find $f_{\rm NL} = 171^{+140}_{-139}$ at 68% C.L. and $-69 < f_{\rm NL} < +492$ at 95% C.L. We discuss the degeneracies between $f_{\rm NL}$ and other cosmological parameters. Including SN-Ia data and priors on H_0 from Hubble Space Telescope observations we find a stronger bound: $-35 < f_{\rm NL} < +479$ at 95%. We also fit the more recent SDSS DR7 halo power spectrum data finding, for a ΛCDM + $f_{\rm NL}$ model, $f_{\rm NL} = -93 \pm 128$ at 68% C.L. and $-327 < f_{\rm NL} < +177$ at 95% C.L. We finally forecast the constraints on $f_{\rm NL}$ from future surveys as EUCLID and from CMB missions as Planck showing that their combined analysis could detect $f_{\rm NL} \sim 5$.

DOI: 10.1103/PhysRevD.82.083511 PACS numbers: 98.80.Cq, 95.35.+d

I. INTRODUCTION

The standard paradigm of structure formation relies on the inflation [1–4], and, as shown in [5–9], it predicts flatness of the Universe and nearly scale-invariant spectrum of initial fluctuations. According to this scenario, quantum-mechanical fluctuations in the scalar field driving inflation lead to primordial density perturbations responsible for the large-scale structures we observe today. Although the simplest assumption is that these fluctuations were Gaussian distributed [10], there are several inflationary models [11–16] involving the existence of a primordial non-Gaussianity. A detection or exclusion of non-Gaussianities would hence be of fundamental interest for understanding the physics of the primordial Universe. Several cosmological observables and methods can be used to constrain non-Gaussianities. Cosmic microwave background (CMB) anisotropies provide the most direct method for the detection of primordial non-Gaussianity (see e.g. [17]) through, for example, measurements of the three-point correlation function [18] (or equivalently the bispectrum) which is nonzero in the presence of non-Gaussianities. The large-scale structure of the Universe is also affected by non-Gaussianities that may be detected by looking at the bispectrum or the trispectrum of galaxy distribution. The abundance of galaxy clusters, that depends on the tails of the density probability distribution, is also sensitive to any deviation from Gaussianity. Non-Gaussianity has a direct impact on the clustering of dark matter halos by changing their mass and correlation function [19–24]. A common way to parametrize primordial non-Gaussianities is to introduce a quadratic correction to the potential [25,26]:

$$\Phi = \phi + f_{\rm NL}(\phi^2 - \langle\phi^2\rangle), \tag{1}$$

where Φ is the primordial potential and ϕ is a Gaussian random field. In this case the non-Gaussianity is a local type correction whose amplitude is given by $f_{\rm NL}$. The most recent constraint on $f_{\rm NL}$ from CMB gives $-10 < f_{\rm NL} < +74$ at 95% C.L. from bispectrum analysis of WMAP-7 years data [27], improving the WMAP5 constrain ($-9 < f_{\rm NL} < +111$) [28]. The authors of [29] used a different estimator applied to WMAP5 data, finding $f_{\rm NL} = -13 \pm 62$ at 68% C.L., while [30], using the needlet bispectrum applied to the same data, found $f_{\rm NL} = +84 \pm 40$ at 68% C.L.

In [24,31–34] it has been shown that a quadratic correction to the potential like that of Eq. (1) produces a scale dependence in the bias of the galaxy clustering with respect to matter distribution. In particular, a scale-dependent term $\Delta b(k)$ arises in the halo bias on larger scales (smaller k) and is proportional to $f_{\rm NL}$ [$\Delta b(k) \propto f_{\rm NL}/k^2$] hence with galaxies being more (less) clustered for positive (negative) values of $f_{\rm NL}$. The authors of [34] analyzed the galaxy power spectrum of luminous red galaxies (LRG) of the Sloan Digital Sky Survey (SDSS) to constrain this scale dependence of the bias, putting the constraint $-21 < f_{\rm NL} < +209$ at 95% C.L. In the same work other large-scale data sets have been used to constrain non-Gaussianity (quasars, integrated Sachs-Wolfe effect data and photometric LRG sample) finding $-29 < f_{\rm NL} < +70$ at 95% C.L. from the combination of all data sets. Recently, the authors of [35] obtained $+25 < f_{\rm NL} < +117$ at 95% C.L. from the combination of WMAP-7 years data [27], baryonic oscillations data from SDSS and Two-degree Field Galaxy Redshift Survey (2dFGRS) [36] and supernovae distance moduli measurements [37] with autocorrelation

function measurements of radio sources from the NRAO VLA Sky Survey [38], claiming a detection of non-Gaussianity at $\sim 3\sigma$.

In this paper we follow the methodology of [34] and constrain $f_{\rm NL}$ by looking at the scale dependence of the bias in current galaxy surveys data. We implement the calculation of galaxy and halo power spectrum using the halo model (see [39] and Sec. II) and we include in it the non-Gaussian scale-dependent correction to the bias. We then place constraints on $f_{\rm NL}$ by comparing this model to the SDSS [40] galaxy power spectrum data [41] and to the halo power spectrum data obtained from the LRG sample [42]. We include in the analysis the WMAP-7 years cosmic microwave background anisotropy data [27]. We also fit the LRG galaxy power spectrum data to the same model, including Hubble constant measurements from the Hubble Space Telescope (HST, [43]) and supernovae distance moduli measurements for the Union data set [37]. Results are shown in Sec. III. We finally forecast the power of future galaxy surveys in constraining non-Gaussianity by generating mock data for galaxy power spectrum using specifications of the EUCLID [44] survey combined with mock data from the Planck [45] satellite and showing in Sec. IV that the combination of data from these experiments could reach the precision required to detect even small non-Gaussianities.

II. HALO MODEL

In the halo-model scenario (see [39] for a detailed review) all matter is contained in halos and, as a consequence, the abundance of halos, their spatial distribution, and their internal density profiles are closely connected to the initial dark matter fluctuation field. Under the assumption that galaxies are formed in these halos of dark matter [46] it is then possible to use the halo model to calculate the statistical properties of the distribution of galaxies. To this aim, the basic quantity is the halo occupation distribution (HOD, see [47]) that encodes the information on how galaxies populate dark matter halos as a function of halo mass. The statistical information is contained in the two-point correlation function of galaxies or equivalently its Fourier transform, the galaxy power spectrum. It is hence important to assess the number of pairs of galaxies in an individual halo and the number of pairs of galaxies in separate halos. The former can be shown to be related to the variance of the HOD, $\sigma^2(M,z) = \langle N_g(N_g-1)\rangle$, while the latter is the square of the mean halo occupation number $N(M,z) = \langle N_g\rangle$. The galaxy power spectrum is then the sum of the 1-halo term describing pairs of objects in the same halo and of a 2-halo term for objects in different halos: $P(k,z) = P_{1h}(k,z) + P_{2h}(k,z)$. The two terms can be written as

$$P_{1h}(k,z) = \frac{1}{n_{\rm gal}^2(z)}\int dM n_{\rm halo}(M,z)|u_{\rm DM}(k,M,z)|^p \times \sigma^2(M,z), \quad (2)$$

$$P_{2h}(k,z) = \frac{P_0(k,z)}{n_{\rm gal}^2(z)}\left[\int dM n_{\rm halo}(M,z)N(M,z) \times b(M,z)u_{\rm DM}(k,M,z)\right]^2, \quad (3)$$

where $n_{\rm halo}$ is the halo mass function [48], $u_{\rm DM}(k,M,z)$ is the normalized dark matter halo density profile in Fourier space, $P_0(k,z)$ is the linear dark matter power spectrum, $b(M,z)$ the linear bias parameter, and $n_{\rm gal}$ is the mean galaxy number per unit of comoving volume:

$$n_{\rm gal}(z) = \int dM n_{\rm halo}(M,z)N(M,z).$$

For low occupied halos [$N(M,z) < 1$] the exponent p of the density profile in Eq. (2) is equal to 1 while it is equal to 2 otherwise [39]. To calculate the two terms (2) and (3) it is necessary to assume a form for the HOD. We choose the parametrization described in [49,50] where the HOD consists of two separated contributions for central and for satellite galaxies:

$$\langle N_{\rm cen}(M)\rangle = \frac{1}{2}Erfc\left[\frac{\ln(M_{\rm min}/M)}{\sqrt{2}\sigma_{\rm cen}}\right], \quad (4)$$

$$\langle N_{\rm sat}(M)\rangle = \left[\frac{M-\gamma M_{\rm min}}{M_1}\right]^{\alpha}, \quad (5)$$

where $M_{\rm min}$, M_1 $\sigma_{\rm cen}$, γ, and α are free parameters of the model. In this description the mean occupation number of central galaxies is modeled as a smoothed step function above the minimum mass $M_{\rm min}$, while satellite galaxies follow a Poisson distribution with a mean given by a power low and a cutoff at multiple γ of the minimum mass. This 5-parameters model showed a good agreement with hydrodynamical and N-body simulations and semianalytic models [51–53].

For the halo density profile $u_{\rm DM}(k,M,z)$, we choose the shape of the Navarro, Frenk, and White profile (NFW) [54]. The variance of the HOD can be calculated as in [55]:

$$\sigma(M,z) = N(M,z), \qquad N(M,z) > 1, \quad (6)$$

$$\sigma(M,z) = \beta(M)^2 N(M,z), \qquad N(M,z) < 1, \quad (7)$$

with $\beta(M,z) = \log_{10}(M/M_{\rm min})/\log_{10}(M_0/M_{\rm min})$ and M_0 is the mass at which the mean occupation number is equal to 1. This parametrization of $\sigma(M,z)$ has been shown to have a good agreement with both semianalytic models and hydrodynamical simulations [56,57]. The halo mass function is given by the Press and Schechter relation [58]:

$$\frac{M^2 n_{\rm halo}(M,z)}{\bar{\rho}}\frac{dM}{M} = \nu f(\nu)\frac{d\nu}{\nu}, \quad (8)$$

where $\bar{\rho}$ is the background comoving density and ν is defined as the ratio between the critical density required for spherical collapse at redshift z [$\delta_{\rm sc}(z)$] and the variance of the initial density fluctuation field $\sigma_0(M)$: $\nu = \delta_{\rm sc}^2(z)/\sigma_0^2(M)$. Here we choose the Sheth-Tormen model [59] for the shape of $\nu f(\nu)$:

$$\nu f(\nu) = A(p)(1 + (q\nu)^{-p})\left(\frac{q\nu}{2\pi}\right)^{1/2} \exp\left(-\frac{q\nu}{2}\right) \quad (9)$$

with $p \sim 0.3$, $A(p) \sim 0.3222$, and $q \sim 0.75$. The linear bias $b(M, z)$ is then given by [59,60]

$$b(M, z) = 1 + \frac{q\nu - 1}{\delta_{sc}(z)} + \frac{2p/\delta_{sc}(z)}{1 + (q\nu)^p}. \quad (10)$$

A. Non-Gaussian corrections

The halo model described so far allows the calculation of the galaxy power spectrum starting from the assumption of Gaussian primordial fluctuations. The existence of deviations from Gaussianity determines a correlation between small-scale and large-scale perturbations because of the quadratic correction $f_{NL}\phi^2$ (in the case of local non-Gaussianities we are considering here) that appear in the potential [25,61]. As shown in [31,33,34] the effect of non-Gaussian fluctuations on the galaxy power spectrum appears on large scales through a scale-dependent correction of the halo bias. Following [34] we write this correction as

$$\Delta b(M, z, k) = \frac{3\Omega_m H_0^2}{c^2 k^2 T(k) G(z)} f_{NL} \frac{\partial \ln n_{halo}}{\partial \ln \sigma_8} \quad (11)$$

that reduces to

$$\Delta b(M, z, k) = \frac{3\Omega_m H_0^2}{c^2 k^2 T(k) G(z)} f_{NL}(b - r)\delta_{sc}, \quad (12)$$

where $G(z)$ is the linear growth factor, $T(k)$ is the transfer function, and the parameter r is 1 if the objects equally populate all the halos, that is a good assumption for the LRG galaxies we use in this analysis (see also [34]) or ~ 1.6 for objects populating only recently merged halos. The information on f_{NL} is then expected to come from the low-k part of the galaxy power spectrum because of the k^{-2} term of Eq. (12) [$T(k)$ is constant at low wave vectors].

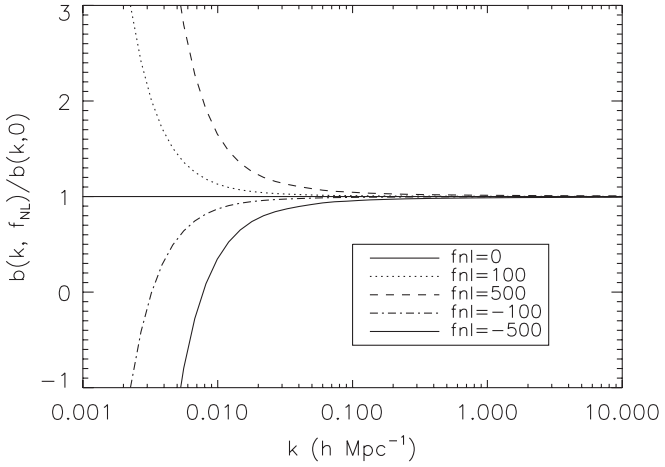

FIG. 1. Scale-dependent correction to the halo bias according to Eq. (12) for different values of f_{NL}.

For an even quite large value of f_{NL}, for example $f_{NL} = +100$, the correction on the halo bias is smaller than a 10% for wave vectors $k > 0.01h$ Mpc^{-1} (see Fig. 1). The amplitude of the correction is proportional to f_{NL} but also to H_0 and Ω_m. One should expect hence important degeneracies among these parameters that will affect the strength of constraints on f_{NL}.

III. ANALYSIS AND RESULTS

A. Constraints from red luminous galaxies power spectra

We implemented the calculation of the theoretical galaxy power spectrum through the halo model described above and performed a Monte Carlo Markov chain analysis using cosmic microwave background data from WMAP-7 years of observations [27] and the most recent LRG galaxy power spectrum data [41] available from the Sloan Digital Sky Survey at a mean redshift $z \simeq 0.35$. We fitted these data assuming flatness of the Universe over a 13 parameters model that consists of 7 standard cosmological parameters (the physical baryon and cold dark matter densities, the ratio of sound horizon to the angular diameter distance at decoupling, the optical depth to reionization, the scalar spectral index, the overall normalization of the spectrum at $k = 0.002h$ Mpc^{-1}, and the amplitude of the Sunyaev-Zel'dovich (SZ) spectrum: $\Omega_b h^2$, $\Omega_c h^2$, θ, τ, n_s, $\log_{10}10^{10}A_s$, and A_{SZ}) and of the 5 parameters of the halo model plus the non-Gaussianity parameter ($\log_{10}M_{min}$, α, γ, σ_{cen}, $\log_{10}M_1$, f_{NL}). In what follows we will express the masses in units of solar masses. The Markov chain analysis has been performed using the publicly available cosmological code COSMOMC [62] suitably modified to include the calculation of the halo model and to fit over the parameters of the halo model and f_{NL}. The convergence diagnostic of this code is based on the Gelman and Rubin statistic [63] (also known as the $R - 1$ statistic, where R is defined as the ratio between the variance of chain means and the mean of variances). The results of our fit are shown in Table I and Fig. 3. For this model we found weak constraints on the non-Gaussianity, $f_{NL} = 171^{+140}_{-139}$ at 68% C.L. and a range $-69 < f_{NL} < +492$ at 95% C.L. from the combination WMAP7 and LRG galaxy power spectrum. The best fit power spectrum computed for the values of Table I is shown in Fig. 2; as one can see there is a slight preference for a nonzero value of f_{NL} at 1σ but is largely consistent with Gaussian initial conditions when we consider 2σ constraints. These limits are weaker than those obtained with a similar data set in [34] where small-scale nonlinearities are modeled with a two parameter k dependent correction. The difference is that in our case the uncertainty on f_{NL} is heavily affected by degeneracies with Ω_m, H_0, and σ_8, parameters which are themselves degenerate with the parameters of the halo model. We are in fact requiring the information on f_{NL} to come only from SDSS data since we are using WMAP data only to constrain cosmological

TABLE I. Best fit values and 68% C.L. errors on the parameters of our model for WMAP7 + LRG and WMAP7 + LRG + SNe + HST data. The combination with SNe and HST data only slightly improves the constraints.

	WMAP7 + LRG	WMAP7 + LRG +HST + SNe
$10^2\Omega_b h^2$	$2.241^{+0.065}_{-0.063}$	$2.263^{+0.055}_{-0.054}$
$\Omega_c h^2$	$0.1103^{+0.0047}_{-0.0047}$	$0.1123^{+0.0036}_{-0.0035}$
θ	$0.010\,395^{+0.000\,032}_{-0.000\,030}$	$0.010\,396^{+0.000\,028}_{-0.000\,027}$
τ	$0.088^{+0.0075}_{-0.0087}$	$0.087^{+0.0065}_{-0.0072}$
n_s	$0.964^{+0.014}_{-0.015}$	$0.965^{+0.012}_{-0.013}$
$\ln(10^{10}A_s)$	$3.08^{+0.04}_{-0.03}$	$3.08^{+0.03}_{-0.03}$
h	$0.715^{+0.023}_{-0.021}$	$0.705^{+0.016}_{-0.015}$
σ_8	$0.800^{+0.028}_{-0.029}$	$0.812^{+0.025}_{-0.025}$
$\log(M_{\rm min})$	$13.90^{+0.16}_{-0.25}$	$14.19^{+0.12}_{-0.12}$
α	$0.85^{+0.18}_{-0.20}$	$0.83^{+0.17}_{-0.18}$
γ	$9.97^{+5.5}_{-5.6}$	$10.7^{+5.1}_{-5.1}$
$\sigma_{\rm cen}$	$1.00^{+0.57}_{-0.57}$	$1.09^{+0.56}_{-0.56}$
$\log(M_1)$	$12.0^{+2.7}_{-2.6}$	$12.3^{+2.7}_{-2.6}$
$f_{\rm NL}$	171^{+140}_{-139}	202^{+129}_{-130}

parameters. The LRG data range only for scales between $0.01 < k < 0.2h$ Mpc^{-1} and, as shown in Fig. 2, on these scales the effect of an even large non-Gaussianity is small and can be easily confused with the effect of cosmological or halo-model parameters. We repeated this fit including both the Hubble Space Telescope prior on H_0 from [43] and supernovae distance moduli measurements for the Union data set [37] obtaining only a slightly improved constraint on $f_{\rm NL}$, i.e. $-35 < f_{\rm NL} < +479$ at 95%, and

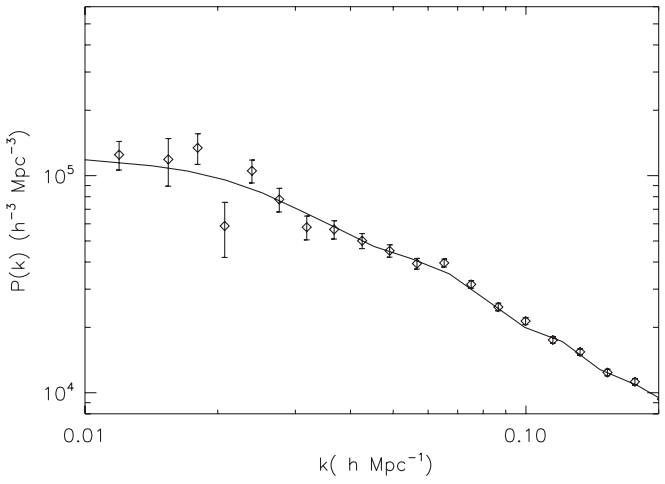

FIG. 2. Best fit galaxy power spectrum calculated with the values of Table I for the fit to WMAP7 + LRG data compared with the LRG galaxy power spectrum.

other parameters. In Fig. 3 we plot constraints on $f_{\rm NL}$ and on the parameters most involved in degeneracies with $f_{\rm NL}$ for the fit to WMAP7 + LRG + SNe + HST data. As for the model parameters, we found generally higher values for $\log_{10}M_{\rm min}$, γ, and $\sigma_{\rm cen}$ than [49], but with greater uncertainty, while α results to be in good agreement and $\log_{10}M_1$ has a very large uncertainty. These differences may arise because of the different data set and modeling (in [49] they fit the projected correlation function) and parameter space. The same figure confirms the expected degeneracy between Ω_m and $\log_{10}M_{\rm min}$ as found also in [49], due to the correlation between halo masses and the number of galaxies in massive halos [64], [65]. The consequence of this degeneracy is that our constraint on the matter density is $\Omega_m = 0.264 \pm 0.022$ from WMAP7 + LRG and hence only slightly better than the constrain from WMAP7 alone $\Omega_m = 0.266 \pm 0.029$.

B. Constraints from halo power spectra

In this section we constrain $f_{\rm NL}$ using recent data of the power spectrum for the reconstructed halo density field derived from a sample of LRGs [42] in the seventh data release of the SDSS (DR7). The halo power spectrum is more directly connected to a dark matter density field for a wider k range and this allows one to use data points in the power spectrum up to $k \sim 0.2h$ Mpc^{-1}. The main difference with respect to the analysis of the previous section is that to model the halo power spectrum it is not necessary to model the halo occupation distribution of galaxies. The halo power spectrum in [42] is modeled as

$$P_{\rm halo}(k) = P_{\rm damp}(k) r_{\rm DM,damp}(k) r_{\rm halo}(k) F_n(k), \qquad (13)$$

where $P_{\rm damp}$ is a power spectrum that account for damping of baryonic acoustic oscillations and is calculated as

$$P_{\rm damp}(k) = P_0(k) e^{-k^2\sigma^2/2} + P_{nw}(k)(1 - e^{-k^2\sigma^2/2}) \qquad (14)$$

with P_0 being the linear matter power spectrum and P_{nw} is the matter power spectrum with baryon oscillations removed calculated as in [66]. The value of σ is chosen fitting the reconstructed halo density field in the mock LRG catalog [42,67]. The factor $F_n(k)$ is a nuisance term defined as

$$F_n(k) = b_0^2\left(1 + a_1\left(\frac{k}{k_*}\right) + a_2\left(\frac{k}{k_*}\right)^2\right), \qquad (15)$$

where b_0 is the effective bias of the LRG at the effective redshift $z_{\rm eff} = 0.313$ and $k_* = 0.2h$ Mpc^{-2}. The likelihood code for halo power spectra for SDSS-DR7 is implemented in COSMOMC and performs a marginalization over the nuisance parameters b_0, a_1, and a_2. The terms $r_{\rm DM,damp}(k)$ and $r_{\rm halo}(k)$ in (13) model the connection between the nonlinear matter power spectrum and the damped linear power spectrum and between halo and matter power spectrum and they are calibrated against

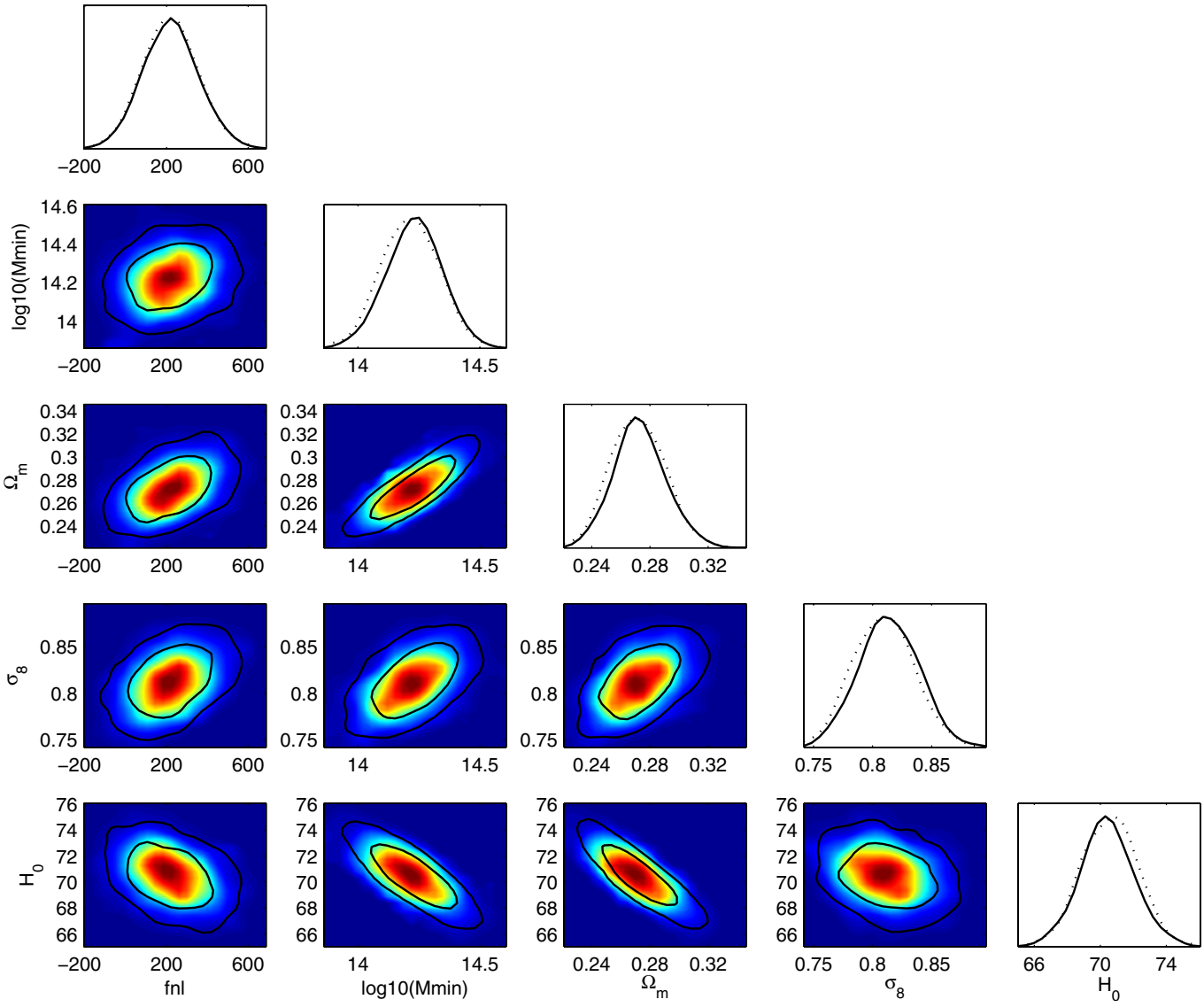

FIG. 3 (color online). 68% and 95% C.L. contour plots and likelihoods for $f_{\rm NL}$ and other parameters of the model for the fit to SDSS DR4 galaxy power spectrum combined with WMAP7, SNe, and HST data. The plot shows the degeneracies of $f_{\rm NL}$ with cosmological and halo-model parameters. As expected $f_{\rm NL}$ results in being correlated with matter density and the Hubble parameter. Strong degeneracies involve also $M_{\rm min}$, Ω_m, σ_8, and H_0 weakening the constraints on these parameters.

numerical simulations (see Sec. 3 in [42] for more details). Here we use a modified version of the modeling described so far introducing the k dependent bias correction (12) averaged over masses:

$$b(k,z) = \frac{\int [b(M,z) + \Delta b(M,z,k)] n_{\rm halo}(M,z) M dM}{\int n_{\rm halo}(M,z) M dM}. \quad (16)$$

We then fitted the data varying $f_{\rm NL}$ together with the seven cosmological parameters ($\Omega_b h^2$, $\Omega_c h^2$, θ, τ, n_s, $\log_{10}10^{10}A_s$, and $A_{\rm SZ}$) and minimizing the chi square by varying nuisance parameters a_1 and a_2. Our results are shown in Table II and in Fig. 4. We also show our best fit halo power spectra in Fig. 5. Our fit for this data set shows a preference for a negative value $f_{\rm NL} = -93 \pm 128$ at 68% C.L. that allows one to have a better fit to five points in the observed power spectra in the range $(0.03 < k < 0.05)h$ Mpc^{-1}. The uncertainty on this value remains anyway quite large and the 95% C.L. range for $f_{\rm NL}$ is $-327 < f_{\rm NL} < +177$, hence with a very slight improvement with respect to the constraints from the previous data set. For the other cosmological parameters we find a good agreement with results from [27] for WMAP7 combined with halo power spectra of the LRG sample.

We note that, according to degeneracies showed in Fig. 4, allowing for a possible non-Gaussianity implies an increase of uncertainty on some cosmological parameters, namely h and σ_8 with an increase of a $\sim$10% on the 1σ error with respect to ΛCDM case for WMAP7 + LRG and an increase of a $\sim$14% on the error for $\Omega_c h^2$.

TABLE II. Best fit values and 68% C.L. errors on the parameters of our model for the fit to SDSS-DR7 halo power spectra.

$10^2\Omega_b h^2$	$2.248^{+0.055}_{-0.055}$
$\Omega_c h^2$	$0.1144^{+0.0041}_{-0.0041}$
θ	$0.010\,389^{+0.000\,026}_{-0.000\,027}$
τ	$0.086^{+0.0063}_{-0.0072}$
n_s	$0.963^{+0.013}_{-0.013}$
$\ln(10^{10}A_s)$	$3.09^{+0.03}_{-0.03}$
h	$0.694^{+0.018}_{-0.018}$
σ_8	$0.822^{+0.025}_{-0.024}$
$f_{\rm NL}$	-93^{+128}_{-129}

IV. FORECAST FOR FUTURE SURVEYS

In this section we consider constraints on $f_{\rm NL}$ from future data generating mock data sets for both CMB anisotropy and galaxy power spectra. For a galaxy survey the error on the matter power spectrum can be calculated as [68,69]

$$\left(\frac{\sigma_P}{P}\right)^2 = \frac{2\pi^2}{4k^2\Delta k V_{\rm eff}}, \tag{17}$$

where the effective volume of the survey is given by

$$V_{\rm eff} = V\left(\frac{nP}{nP+1}\right)^2 \tag{18}$$

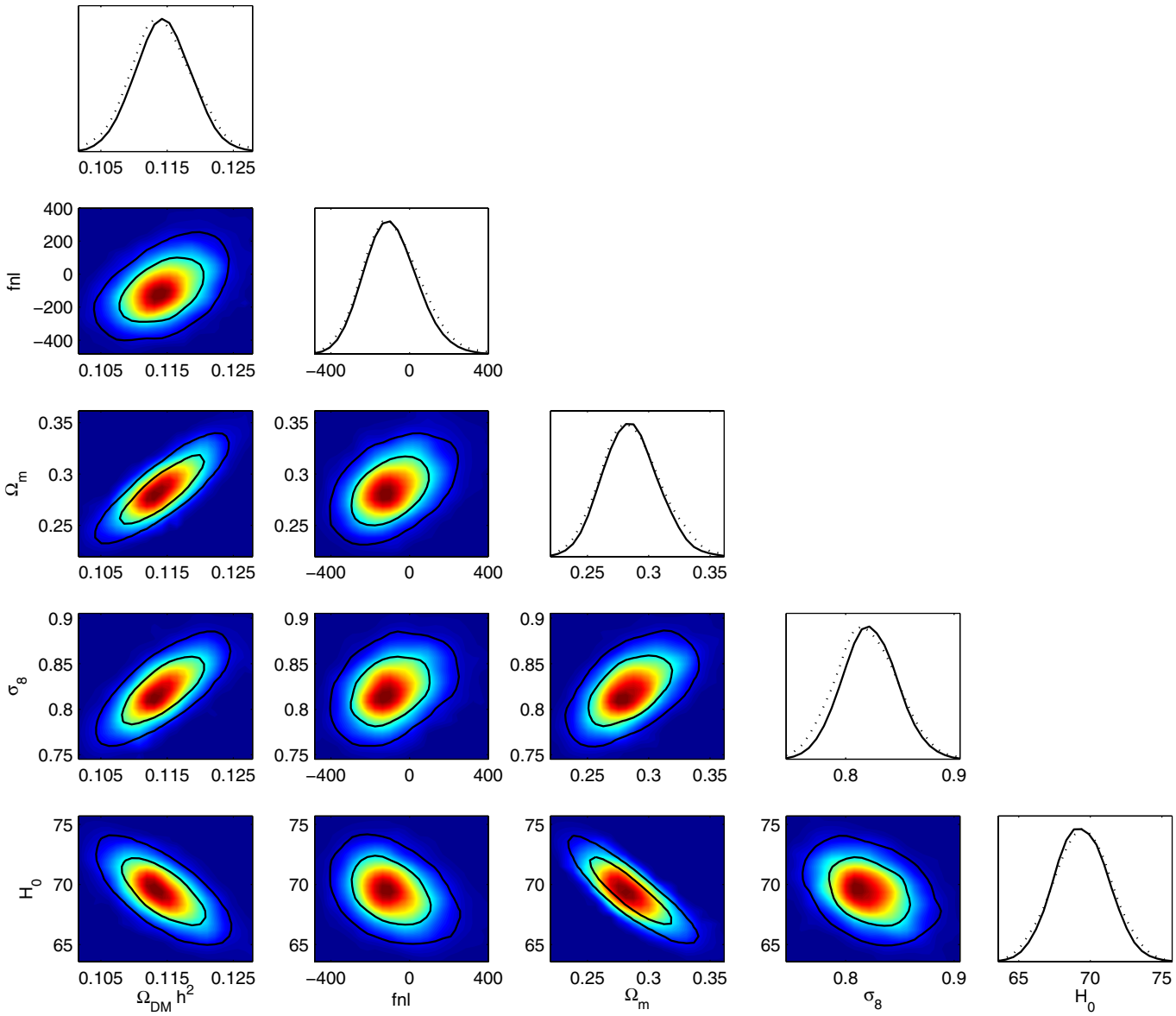

FIG. 4 (color online). 68% and 95% C.L. contour plots and likelihoods for some parameters of our model for the fit to SDSS-DR7 data. As noted before $f_{\rm NL}$ results in being correlated mainly with matter density and the Hubble parameter.

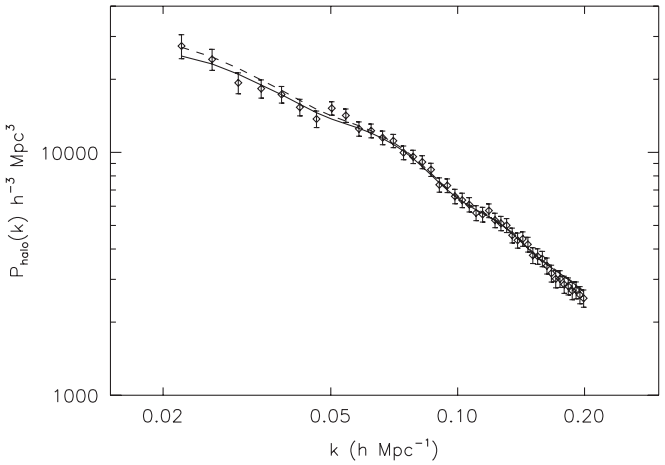

FIG. 5. Best fit model (solid line) to halo power spectra data from SDSS-DR7. We show for comparison the same model but with $f_{\rm NL} = 0$. A negative value of $f_{\rm NL}$ allows one to have a better fit to the data points in the range $(0.03 < k < 0.05)h$ Mpc^{-1}

and Δk is the width of k bins. Here we use specification for a typical future galaxy survey like EUCLID [44] with galaxy number density $n \simeq 1.6 \times 10^{-3}$, redshift range $0 < z < 2$ and $f_{\rm sky} \simeq 0.5$. The minimum k of the mock data set is chosen to be greater than $2\pi/V^{1/3}$, while the maximum k we use is $0.02h$ Mpc^{-1}. For CMB anisotropy power spectrum we use the specification for the Planck experiment [45] assuming the noise of the 143 GHz channel. We explore a ΛCDM + $f_{\rm NL}$ model and we choose as a fiducial model the WMAP-7 years best fit for ΛCDM parameters [27]. For the non-Gaussianity parameter we choose three fiducial models, $f_{\rm NL} = +1$, $+5$, and $+10$. Remember that in our approach we are using only the information of large-scale galaxy clustering to constrain non-Gaussianity, while we use CMB measurements only to constrain other cosmological parameters and hence to break degeneracies.

Results of our forecast on $f_{\rm NL}$ are shown in Table III. As one can see the combination of accurate galaxy power spectrum measurements, attainable with a survey like EUCLID and Planck CMB measurements, could reach the sensitivity required to detect an even small non-Gaussianity, such as $f_{\rm NL} = +5$ or $f_{\rm NL} = +10$, with a confidence level of at least 95%. We note that this results

TABLE III. 1σ errors (68% C.L.) from the combination of mock data sets generated for the specifications of the Planck experiment and the EUCLID survey and for three different fiducial values of $f_{\rm NL}$.

EUCLID + Planck	
Fiducial value	σ
$f_{\rm NL} = +1$	2.23
$f_{\rm NL} = +5$	2.29
$f_{\rm NL} = +10$	2.39

in agreement with other forecasts for future galaxy surveys (see [70] for example). Very small non-Gaussianities ($f_{\rm NL} = +1$) seem instead rather difficult to detect, mainly due to degeneracies with other parameters. Nevertheless in [71] it has also been shown that in more complicated models (allowing variation of neutrino mass, running of spectral index, dark energy equation of state, and relativistic degrees of freedom) constraints on $f_{\rm NL}$ may deteriorate up to $\sim$80%.

V. SYSTEMATICS

Before concluding we discuss the possible systematics introduced by the assumptions we made or, more generally, by the theoretical uncertainties of the model.

First, we have seen that the value of r that appears in Eq. (12) may have a value in the range 1–1.6. We have assumed $r = 1$ since we are using luminous red galaxies that are old galaxies at the center of halos. This is a common assumption for this kind of analysis (see also [34]). Anyway we find that even assuming $r = 1.6$ the differences in the power spectrum with respect to the case $r = 1$ are very small. Using $r = 1.6$ we find only a slight variation in the χ^2 with respect to $r = 1$ for the best fit model: $\Delta\chi^2 \sim 0.3$. The reason for this is that actual data constrain scales $k > 0.02h$ Mpc^{-1} where the exact value of r is less relevant. Nevertheless for future low-k data it may be necessary for a more precise modeling of Eq. (12).

A second assumption we made is that the density profile of the halos is described by the NFW profile. Although the exact shape of the profiles in the halos is still uncertain, this profile has been tested against several numerical simulations and it turned out to be a good approximation [39]. Moreover, again, the information on $f_{\rm NL}$ is coming from $k < 0.1h$ Mpc^{-1} where the density profile is constant in Fourier space.

An important point is the comparison between the results from the LRG power spectrum of [41] and the halo power spectrum from [42]. The first data set provides a galaxy power spectrum while the second a halo density field that does not require any assumption about the halo occupation number. In [42] there is a large discussion on the differences between these two data sets and we refer the reader to this work for a complete discussion. Here we remark that the main differences are due to the heavy Finger of Gods compression algorithm used in [41] to obtain the matter power spectrum. This process may cause transfer of power from a scale to another, causing consistent deviations (up to $\sim$40% on $k = 0.2h$ Mpc^{-1}) between the reconstructed halo density field and the matter power spectrum [42]. For the DR7 halo power spectrum instead, the halo density field is reconstructed before the computation of the power spectrum (see Sec. 2.2 in [42]) and the deviations between the two are smaller than 4%. Also the modeling of the theoretical halo power spectrum and of the galaxy power spectrum is different. The model of

[42] is calibrated on N-body simulations and mock data sets made especially for this LRG sample. Moreover the authors of [42] imposed priors on the nuisance parameters of the model based on N-body simulations. For the galaxy power spectrum of [41] the Q model was used [72] for the nonlinear part of the power spectrum, marginalizing over Q with weak priors. All these differences necessarily reflect on the cosmological parameters estimation, including $f_{\rm NL}$. The comparison between results of the two data sets is made in Sec. 6.1 of [42]. Significant differences are found on some cosmological parameters from the two LRG data sets only (i.e. not including CMB) of the two releases: in particular, the $\Omega_m h$ values [that enter also in Eq. (12)] differ of almost 2σ between the two surveys.

In our work, to fit the DR7 data we are only introducing the bias scale-dependent correction to the model of [42], in order to be as much as possible consistent with the data compression algorithm of this LRG catalog. We ascribe the differences between the results of Secs. III A and III B to the significant differences of the data compression process, as noted also in [42].

The last issue concerns the modeling of power spectra on nonlinear scales. For DR7 data, the authors of [42] normalize the final halo power spectrum using mock catalogs to account for the small offset between the N-body and HALOFIT results.

Concerning the galaxy power spectrum we used to fit data from [41], the $P(k)$ we are using in relation (3) is the linear matter power spectrum, which is well known. The galaxy power spectrum is calculated through the halo model itself. The 5-parameters model we are using showed a good agreement with hydrodynamical and N-body simulations and semianalytic models [51–53,56,57]. Moreover, we are marginalizing over the 5 free parameters that account for the uncertainties of the model, so that our analysis is rather conservative.

In the forecast section we model the galaxy power spectrum relying on the same assumption made above ($r = 1$ for galaxies and NFW profiles) and using the same HOD modeling. Our results show the potential of a survey like EUCLID to detect even small non-Gaussianities and are in good agreement with forecast done for the same survey and for a similar modeling of the scale-dependent bias [70]. It is clear, however that the analysis of real data from these future surveys will probably require a more accurate modeling of the galaxy power spectrum and of the scale-dependent correction in order to not bias the estimated value of the cosmological parameters.

VI. CONCLUSIONS

We place new constraints on the local type non-Gaussianity parameter $f_{\rm NL}$ by looking at the scale dependence of the halo bias (at small wave vectors) in the recent galaxy and halo power spectra measurements from the LRG sample of the Sloan Digital Sky Survey. We fit 2006 SDSS power spectra data with a halo model consisting of 5 parameters plus 7 cosmological parameters and $f_{\rm NL}$. Our large parameter space and the restriction of the data set to relatively small scales ($k > 0.01h$ Mpc^{-1}) lead to a weak constraint: $-69 < f_{\rm NL} < +492$ at 95% C.L. We show and discuss degeneracies with halo model parameters. When including both type Ia supernovae and HST data the 1σ error on $f_{\rm NL}$ is reduced to about $\sim$10%. We use also 2009 halo power spectra data obtained from the SDSS LRG sample finding a slightly better constraint $-327 < f_{\rm NL} < +177$ at 95% C.L., again limited by the fact that the data set does not extend below $k \sim 0.02h$ Mpc^{-1}. We also forecast the constraints obtainable from data sets of a survey like EUCLID when combined with Planck CMB data, finding that these surveys could reach the accuracy required to detect even small non-Gaussianities as $f_{\rm NL} = +5$, thus confirming the power of this method. Finally we discuss the possible systematics and theoretical uncertainties that may affect the results.

ACKNOWLEDGMENTS

F. D. B. thanks the UCI Center for Cosmology for support and hospitality while this research was being conducted. This work was supported by NSF CAREER AST-0645427 and NASA NNX10AD42G at UCI. This research has been partially supported by the ASI/INAF agreement I/072/09/0 for the Planck LFI Activity of Phase E2.

[1] A. A. Starobinskiĭ, Sov. J. Exp. Theor. Phys. Lett. **30**, 682 (1979).
[2] A. H. Guth, Phys. Rev. D **23**, 347 (1981).
[3] A. D. Linde, Phys. Lett. **108B**, 389 (1982).
[4] A. Albrecht and P. J. Steinhardt, Phys. Rev. Lett. **48**, 1220 (1982).
[5] V. F. Mukhanov and G. V. Chibisov, Sov. J. Exp. Theor. Phys. Lett. **33**, 532 (1981).
[6] S. W. Hawking, Phys. Lett. **115B**, 295 (1982).
[7] A. H. Guth and S.-Y. Pi, Phys. Rev. Lett. **49**, 1110 (1982).
[8] A. A. Starobinskij, Phys. Lett. **117B**, 175 (1982).
[9] J. M. Bardeen, P. J. Steinhardt, and M. S. Turner, Phys. Rev. D **28**, 679 (1983).
[10] J. M. Bardeen, J. R. Bond, N. Kaiser, and A. S. Szalay, Astrophys. J. **304**, 15 (1986).
[11] A. Linde and V. Mukhanov, Phys. Rev. D **56**, R535 (1997).
[12] D. H. Lyth and D. Wands, Phys. Lett. B **524**, 5 (2002).

[13] D. H. Lyth, C. Ungarelli, and D. Wands, Phys. Rev. D **67**, 023503 (2003).
[14] F. Vernizzi and D. Wands, J. Cosmol. Astropart. Phys. 05 (2006) 019.
[15] K. A. Malik and D. H. Lyth, J. Cosmol. Astropart. Phys. 09 (2006) 008.
[16] M. Sasaki, J. Valiviita, and D. Wands, Phys. Rev. D **74** 103003 (2006).
[17] N. Bartolo, S. Matarrese, and A. Riotto, arXiv:1001.3957.
[18] S. Matarrese, L. Verde, and A. F. Heavens, Mon. Not. R. Astron. Soc. **290**, 651 (1997).
[19] F. Lucchin, S. Matarrese, and N. Vittorio, Astron. Astrophys. **162**, 13 (1986).
[20] S. Matarrese, L. Verde, and R. Jimenez, Astrophys. J. **541**, 10 (2000).
[21] J. Robinson and J. E. Baker, Mon. Not. R. Astron. Soc. **311**, 781 (2000).
[22] A. J. Benson, C. Reichardt, and M. Kamionkowski, Mon. Not. R. Astron. Soc. **331**, 71 (2002).
[23] R. Scoccimarro, E. Sefusatti, and M. Zaldarriaga, Phys. Rev. D **69**, 103513 (2004).
[24] N. Dalal, O. Dore, D. Huterer, and A. Shirokov, Phys. Rev. D **77**, 123514 (2008).
[25] A. Gangui, F. Lucchin, S. Matarrese, and S. Mollerach, Astrophys. J. **430**, 447 (1994).
[26] E. Komatsu and D. N. Spergel, in *Proceedings*, edited by R. T. Jantzen, V. Gurzadyan, and R. Ruffini (World Scientific, Singapore, 2002), p. 2009.
[27] E. Komatsu *et al.*, arXiv:1001.4538.
[28] E. Komatsu *et al.* (WMAP Collaboration), Astrophys. J. Suppl. Ser. **180**, 330 (2009).
[29] E. Calabrese *et al.*, Phys. Rev. D **81**, 043529 (2010).
[30] O. Rudjord, F. K. Hansen, X. Lan, M. Liguori, D. Marinucci, and S. Matarrese, Astrophys. J. **701**, 369 (2009).
[31] L. Verde, L. M. Wang, A. Heavens, and M. Kamionkowski, Mon. Not. R. Astron. Soc. **313**, 141 (2000).
[32] B. A. Reid, L. Verde, K. Dolag, S. Matarrese, and L. Moscardini, J. Cosmol. Astropart. Phys. 07 (2010) 013.
[33] S. Matarrese and L. Verde, Astrophys. J. **677**, L77 (2008).
[34] A. Slosar, C. Hirata, U. Seljak, S. Ho, and N. Padmanabhan, J. Cosmol. Astropart. Phys. 08 (2008) 031.
[35] J. Q. Xia, M. Viel, C. Baccigalupi, G. De Zotti, S. Matarrese, and L. Verde, Astrophys. J. **717**, L17 (2010).
[36] W. J. Percival *et al.*, Mon. Not. R. Astron. Soc. **401**, 2148 (2010).
[37] M. Kowalski *et al.* (Supernova Cosmology Project Collaboration), Astrophys. J. **686**, 749 (2008).
[38] J. J. Condon, W. D. Cotton, E. W. Greisen, Q. F. Yin, R. A. Perley, G. B. Taylor, and J. J. Broderick, Astron. J. **115**, 1693 (1998).
[39] A. Cooray and R. K. Sheth, Phys. Rep. **372**, 1 (2002).
[40] www.sdss.org.
[41] M. Tegmark *et al.* (SDSS Collaboration), Phys. Rev. D **74**, 123507 (2006).
[42] B. A. Reid *et al.*, Mon. Not. R. Astron. Soc. **404**, 60 (2010).
[43] A. G. Riess *et al.*, Astrophys. J. **699**, 539 (2009).
[44] A. Refregier *et al.*, Proc. SPIE Int. Soc. Opt. Eng. **6265**, 62651Y (2006).
[45] G. Efstathiou, C. Lawrence, J. Tauber, and the Planck Collaboration, arXiv:astro-ph/0604069.
[46] S. D. M. White and M. Rees, Mon. Not. R. Astron. Soc. **183**, 341 (1978); Phys. Rep. **372**, 1 (2002).
[47] J. A. Peacock and R. E. Smith, Mon. Not. R. Astron. Soc. **318**, 1144 (2000).
[48] R. K. Sheth and G. Tormen, Mon. Not. R. Astron. Soc. **329**, 61 (2002).
[49] K. Abazajian *et al.* (SDSS Collaboration), Astrophys. J. **625**, 613 (2005).
[50] Z. Zheng *et al.*, Astrophys. J. **633**, 791 (2005).
[51] J. Guzik and U. Seljak, Mon. Not. R. Astron. Soc. **335**, 311 (2002).
[52] A. A. Berlind *et al.*, Astrophys. J. **593**, 1 (2003).
[53] A. V. Kravtsov, A. A. Berlind, R. H. Wechsler, A. A. Klypin, S. Gottloeber, B. Allgood, and J. R. Primack, Astrophys. J. **609**, 35 (2004).
[54] J. F. Navarro, C. S. Frenk, and S. D. M. White, Astrophys. J. **490**, 493 (1997).
[55] M. Magliocchetti, L. Silva, A. Lapi, G. De Zotti, G. L. Granato, D. Fadda, and L. Danese, Mon. Not. R. Astron. Soc. **375**, 1121 (2007).
[56] M. P. Viero *et al.*, Astrophys. J. **707**, 1766 (2009).
[57] A. A. Berlind and D. H. Weinberg, Astrophys. J. **575**, 587 (2002).
[58] W. H. Press and P. Schechter, Astrophys. J. **187**, 425 (1974).
[59] R. K. Sheth and G. Tormen, Mon. Not. R. Astron. Soc. **308**, 119 (1999).
[60] H. J. Mo, Y. P. Jing, and S. D. M. White, Mon. Not. R. Astron. Soc. **282**, 1096 (1996).
[61] E. Komatsu and D. N. Spergel, Phys. Rev. D **63**, 063002 (2001).
[62] A. Lewis and S. Bridle, Phys. Rev. D **66**, 103511 (2002).
[63] A. Gelman and D. B. Rubin, Stat. Sci. **7**, 457 (1992).
[64] Z. Zheng, J. L. Tinker, D. H. Weinberg, and A. A. Berlind, Astrophys. J. **575**, 617 (2002).
[65] E. Rozo, S. Dodelson, and J. A. Frieman, Phys. Rev. D **70**, 083008 (2004).
[66] D. J. Eisenstein and W. Hu, Astrophys. J. **496**, 605 (1998).
[67] B. A. Reid, D. N. Spergel, and P. Bode, Astrophys. J. **702**, 249 (2009).
[68] H. A. Feldman, N. Kaiser, and J. A. Peacock, Astrophys. J. **426**, 23 (1994).
[69] M. Tegmark, Phys. Rev. Lett. **79**, 3806 (1997).
[70] C. Carbone, L. Verde, and S. Matarrese, Astrophys. J. **684**, L1 (2008).
[71] C. Carbone, O. Mena, and L. Verde, J. Cosmol. Astropart. Phys. 07 (2010) 020.
[72] S. Cole *et al.* (The 2dFGRS Collaboration), Mon. Not. R. Astron. Soc. **362**, 505 (2005).